Macromolecules **1989**, *22*, 2472–2477

(18) SAS Institute, SAS Circle, Box 8000, Carry, NC, 27511.
(19) Havriliak, S., Jr.; Shortridge, T. J. *Plast. Eng.* in press.
(20) Havriliak, S., Jr. *Computer Applications in the Polymer Laboratory*; Provder, T., Ed.; ACS Symposium Series 313; American Chemical Society: Washington, DC, 1986.
(21) Bueche, F. *J. Chem. Phys.* **1953**, *21*, 1850.
(22) Havriliak, S., Jr. *Polymer* **1968**, *9*, 289.
(23) Havriliak, S., Jr.; Roman, N. *Polymer* **1966**, *6*, 387.

Molecular Modeling of Polymers. 6. Intramolecular Conformational Analyses and Molecular Dynamics of Syndiotactic Polystyrene

D. C. Doherty and A. J. Hopfinger*

Department of Chemistry, The University of Illinois at Chicago, P.O. Box 6998, Chicago, Illinois 60680.

Received August 15, 1988; Revised Manuscript Received November 29, 1988

ABSTRACT: Fixed valence geometry molecular mechanics conformational analyses of syndiotactic polystyrene (sPS) were performed. The PRIMM method was employed to measure relative conformational stability as a function of the number of nearest monomer neighbor interactions considered. Only two stable ordered conformations of sPS were identified. These are the all-trans conformation (T_4) and the trans-trans-gauche-gauche (T_2G_2) structure. Two crystalline phases of sPS have been observed. The diffraction pattern of one form has been interpreted in terms of a T_4 chain conformation. The other crystalline phase is postulated to have chains in the T_2G_2 conformation. Preliminary molecular dynamics (MD) simulation studies also indicate that the T_4 and T_2G_2 conformations are the only stable intrachain structures. The interconversion energy barrier between T_2G_2 and T_4 is estimated to be about 2–3 kcal/mol from both conformational analysis and MD simulation. A T_2G_2-to-T_4 transition was observed in the MD trajectory, but not the reverse transition.

Introduction

The recent development of successful schemes for the synthesis of syndiotactic polystyrene, sPS,[3] raises the issue of possible commercial uses of this polymer and/or its homologues. Thus, it is of interest to determine the physicochemical properties of sPS. Similarities of sPS to isotactic polystyrene, iPS, and to other syndiotactic vinyl polymers are of particular interest.

Relatively little information has been published on the physicochemical properties of sPS. Ishihara and coworkers[3] note that the characteristic IR signals in the region 1450–1180 cm^{-1} associated with iPS are absent for sPS. However, a new signal at 1200 cm^{-1} for sPS is attributed to its ordered chain conformation. The crystallization rate of sPS is extremely high compared to iPS. The crystal melt temperature is about 270 °C, about 40 °C higher than iPS.[3]

Two crystalline phases, termed α and β,[5] have been observed for sPS. The α phase has a fiber axis repeat of 5.0–5.1 Å.[3-5] The all-trans chain conformation, T_4, has been postulated for the α phase[3-5] by analogy to other crystalline polymers, such as polyethylene, which have fiber axis repeat units of about half-multiples of 5.0 Å and are in the T_4 chain conformation. The same reasoning has been applied to the β phase of sPS where the fiber axis repeat unit is about 7.5 Å,[5] which is characteristic of a trans-trans-gauche-gauche (T_2G_2) conformation as found, for example, in one of the crystalline forms of syndiotactic polypropylene (sPP).[6] The other crystalline form of sPP is, interestingly, T_4.[7] The α phase is obtained by annealing the melt-quenched glass, while the β form is formed by casting from solution.[4,5] The β form converts to the α phase when heated to 180–190 °C.[5] There is some evidence that two different modes of chain packing occur in the α phase depending upon the method of crystallization.[4]

Table I
Selected Values of θ_1 and θ_2 and the Nearest Structural Repeat Unit Conformational Energies, E_i,[a] for the T_4 and T_2G_2 Conformations

conformation	θ_1	θ_2	E_0	E_1	E_2	E_3	E_p
T_4	109.5°	109.5°	16.45	−3.96	−0.26	−0.02	12.21
	112.0	114.0	14.51	−3.05	−0.23	−0.01	11.22
T_2G_2	109.5	109.5	18.89	0.07	33.43	−0.26	52.13
	112.0	114.0	15.73	−1.15	−2.79	−0.23	11.56

[a] In kcal/mol/structural repeat unit. [b] E_p is the energy of the infinite polymer using up to three nearest structural repeat unit interactions.

Since there has not been extensive structural characterization of sPS, we thought that this might be a good opportunity to use computer-aided molecular modeling[8] to predict some properties of sPS that might facilitate corresponding laboratory experiments.

This paper reports the results of the intrachain conformational analyses of sPS. Subsequent papers will deal with the characterization of the intermolecular structure of sPS.

Method

The repeat unit geometry used in the conformational analyses of sPS is shown in Figure 1. The equivalence rule[1] was applied in the conformational analyses and is based upon the structural (as opposed to chemical) repeat unit geometry. With the exception of the backbone bond angles θ_1 and θ_2, all other bond lengths and angles were assigned standard values. The choices in θ_1 and θ_2 are given in Table I and are based upon suggested values for iPS.[2,9,10] There have been different viewpoints regarding what values of θ_1 and θ_2 best fit the crystal data for iPS. The strategy in our choosing different θ_1 and θ_2 is to hypothesize that these variables may also be problematic for sPS and to see how sensitive the conformational profiles of sPS are

---

* To whom all correspondence should be addressed.

0024-9297/89/2222-2472$01.50/0

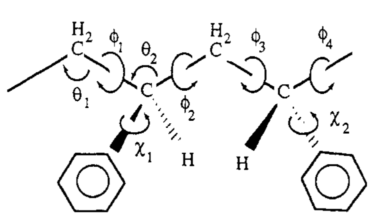

Figure 1. Structural repeat unit for sPS with backbone and torsion angles defined.

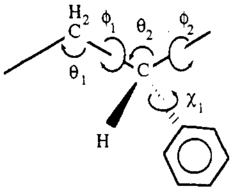

Figure 2. Same as Figure 1 but for iPS.

to these particular geometric variables.

Fixed valence geometry molecular mechanics was selected to perform the intramolecular conformational analyses of sPS.[1] In addition, the PRIMM method[2] was used in assigning the structural repeat unit contributions to the conformational energy. This formalism makes it possible to correctly determine the contributions of different nearest unit neighbor interactions on the stability of ordered conformations of linear chain segments. It is also possible to estimate the relative stability of a particular conformational state adopted by different oligomers and high polymers using the PRIMM method.

The form of the force field used in the conformational analyses is

$$P(\phi_1,\phi_2,\phi_3,\phi_4,\chi_1,\chi_2,\theta_1,\theta_2) = \sum_i \sum_j \left[\frac{-a_{ij}}{{r_{ij}}^6} + \frac{b_{ij}}{{r_{ij}}^{12}} + C\frac{Q_iQ_j}{\epsilon r_{ij}} \right] + \sum_m [\sum_{l=1}^{4} T(\phi_1) + \sum_{k=1}^{2} T(\chi_k)] \tag{1}$$

The Q_α's are the partial atomic charges as determined from CNDO/2 calculations[11] on a trimer repeat unit. The Q_α's of the middle monomer unit of the trimer are used to represent all monomers. A fixed molecular dielectric of $\epsilon = 3.5$ was used throughout the study, and C is an energy units conversion constant. The $T(\phi_k)$ and $T(\chi_k)$ are the intrinsic torsional potentials, which were selected from the CHEMLAB-II library of torsional potential functions.[12] The r_{ij}'s are the distances between pairs of atoms, which are a function of at least one torsion angle.

A major concern in the study was the selection of an appropriate set of nonbonded potentials—the a_{ij}'s and b_{ij}'s of eq 1. It was decided that the criterion for selecting the nonbonded potential set would be to reproduce the 3_1 helical conformation of crystalline iPS[10] as an intramolecular energy minimum. The repeat unit geometry for iPS is shown in Figure 2. Conformational analyses were carried out on iPS as a function of $(\phi_1,\phi_2,\chi_1,\theta_1,\theta_2)$ and N, the number of nearest repeat unit neighbor interactions for three different sets of potentials. ϕ_1, ϕ_2, and χ_1 were scanned at a resolution of 30°. By symmetry, χ_1 was only explored over a 180° rotation range. We also took advantage of symmetry for ϕ_1 or ϕ_2 and explored each of these torsion angles between cis and trans states.

The three potential sets considered were (a) a set proposed by Flory and co-workers,[9] another developed by Hopfinger,[1] and the 6–12 equivalents to the nonbonded potentials of the MM2 force field.[13] Succinctly, the Hopfinger potentials are too soft and stabilize the all-trans conformation of iPS at the expense of other conformations, while the MM2 potentials are too hard and predict the 3_1 helix to be unstable. The Flory potentials, however, do predict the 3_1 helix to be the global intramolecular energy minimum for $N = 1$–6 for iPS. The conformational energy map of ϕ_1 versus ϕ_2 with the energy minimized with respect to χ_1 and $N = 6$ for the Flory potentials is shown in Figure 3. The conformational energy profiles are sensitive to the selection of θ_1 and θ_2 as found for iPS. The values of θ_1 and θ_2 to construct Figure 3 are 112° and 114°. This sensitivity of chain conformation to θ_1 and θ_2 is expanded upon below in the Results section.

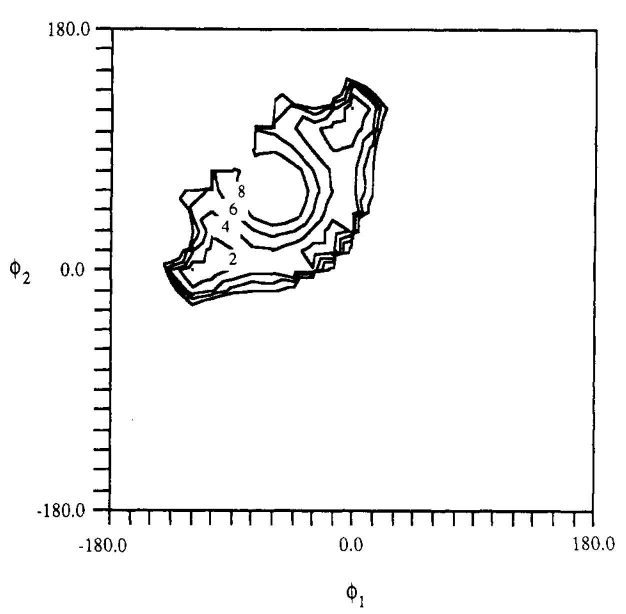

Figure 3. Conformational energy map using the Flory potentials for iPS with χ_1 optimized at each point. $N = 6$ and the energy contours are in kilocalories/mole relative to the global minimum denoted by •. $\phi_1 = \phi_2 = 0°$ corresponds to the all-trans conformation.

The conformational analyses of sPS were carried out using the Flory potentials. The set of torsion angles of the repeat unit geometry, shown in Figure 1, was initially explored at 30° scanning resolution. We took advantage of torsion angle symmetry whenever possible to minimize the number of conformations that had to be sampled. Nevertheless, 746 496 conformations had to be considered in the initial conformational scan. The apparent minima were identified for the 30° scan resolution analysis, and these apparent minima were refined to 5° scan resolution by systematically searching throughout the conformational space within ±30° of each apparent minimum torsion angle value. N was allowed to vary from 1 to 3 in order to evaluate the role of longer range interactions upon relative conformer stability. It should be remembered that N is defined differently for iPS and sPS because of the different structural repeat units.

Results

Table I contains the results of the conformational analyses as a function of N, θ_1, and θ_2. The key finding is that only two ordered chain conformations of sPS are found. The all-trans (T_4) conformation is found to be the most stable, which is consistent with limited experimental data.[3-5] However, its relative stability decreases as N increases when compared to the other stable conformer—a trans–trans–gauche–gauche (T_2G_2) structure. The intramolecular conformational energies for T_4 and T_2G_2 of sPS are given as part of Table I. Rotations of the phenyl rings, χ_1 and χ_2, are quite restricted in sPS in a manner similar to iPS. The lowest energy conformer state for T_4 corre-

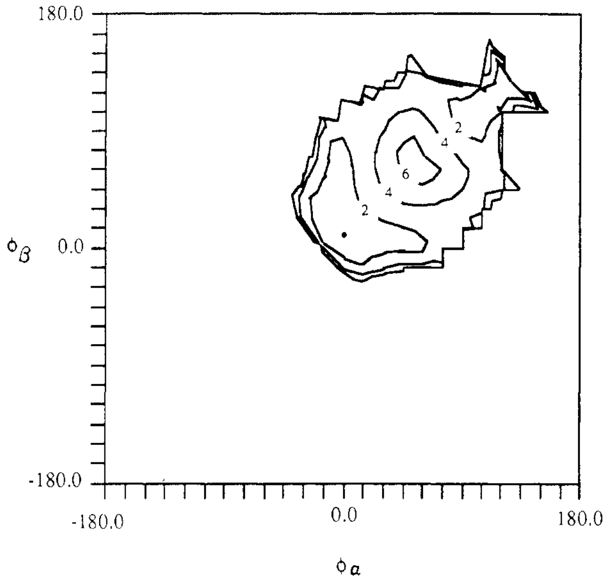

Figure 4. Same as Figure 3 but for sPS with $\phi_1 = \phi_5 = \phi_9 = \phi_\alpha$ and $\phi_2 = \phi_6 = \phi_{10} = \phi_\beta$.

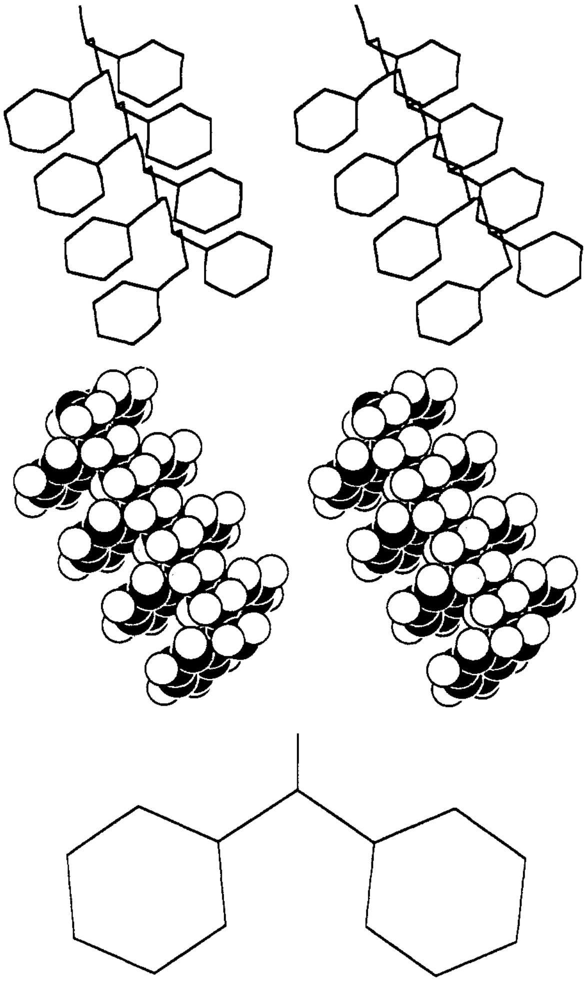

Figure 5. All-trans, T_4, conformation of sPS: (a, top) stick stereo, (b, middle) space-fill stereo, (c, bottom) projected along the chain axis.

sponds to the rings that are perpendicular to the chain axis. The preferred conformation for the T_2G_2 structure has the same relative torsion angle values, $(\chi_1,\chi_2) = (\pm 60°, \mp 60°)$, found for T_4. However, the rings have different orientations with respect to the chain axis for T_2G_2 than for T_4, owing to the change in backbone conformation.

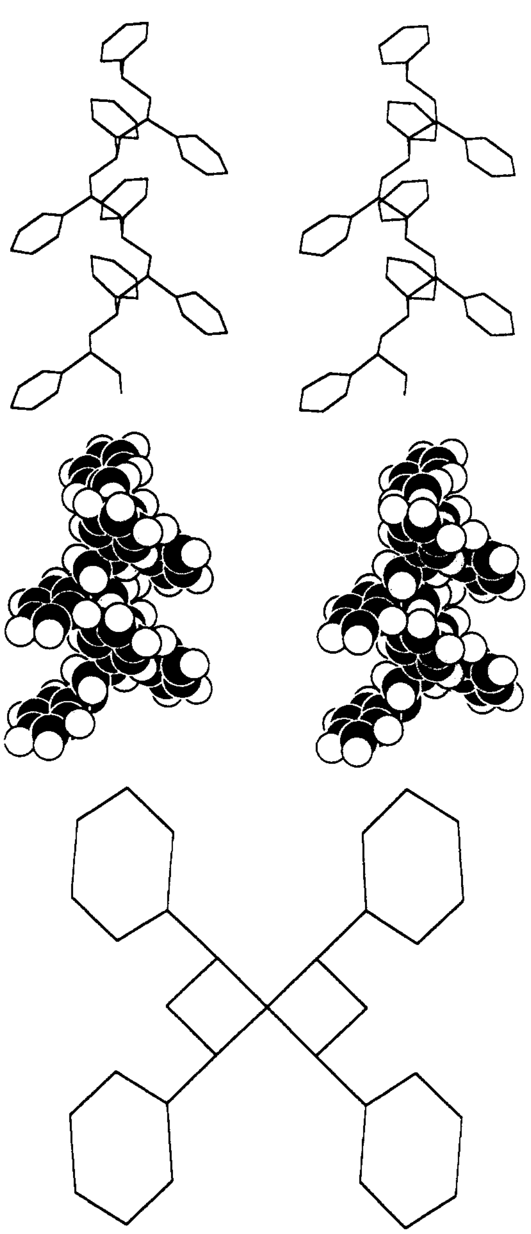

Figure 6. T_2G_2 conformation of sPS: (a, top) stick stereo, (b, middle) space-fill stereo, (c, bottom) projected along the chain axis.

Our findings suggest that, for semiordered samples of sPS, short chain segments of an all-trans conformation would be preferred over T_2G_2 conformational segments. A conformational energy map of $\phi_1 = \phi_5 = \phi_9 = \phi_\alpha$ versus $\phi_2 = \phi_6 = \phi_{10} = \phi_\beta$ is presented in Figure 4 for $N = 3$. This map presents partial, but representative, information on the relative conformational profile of sPS. The T_4 conformation corresponds to $\phi_\alpha = \phi_\beta = 0°$ and is the global energy minimum. The T_2G_2 conformation is located at $\phi_\alpha = \phi_\beta = 240°$. The choice of isomers used in the conformational analysis dictate whether the T_2G_2 conformation will be a secondary minimum at $\phi_\alpha = \phi_\beta = 240°$ or at $\phi_\alpha = \phi_\beta = 120°$. The torsion angles ϕ_3, ϕ_4, ϕ_1, and ϕ_2, and their segment monomer equivalents, are the same for T_4 and T_2G_2. The partial conformational profile expressed in the energy map of Figure 4 indicates that there are low-energy interconversion pathways between T_4 and T_2G_2. The interconversion barriers are 2–3 kcal/mol. Figures 5 and 6 display the T_4 and T_2G_2 conformations, respectively, in stereo stick and space-fill representations.

The conformational profiles of sPS are found to be dependent upon the values of θ_1 and θ_2. This can be seen

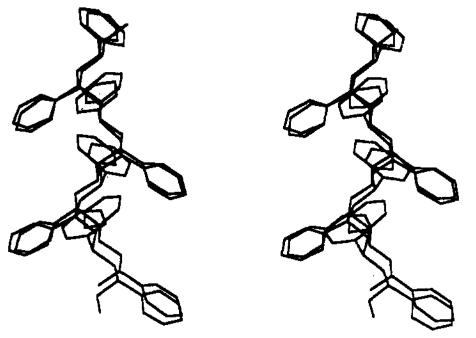

Figure 7. Variation in T_2G_2 conformation as a result of changing (θ_1,θ_2) from (109.5°,109.5°) to (112°,114°).

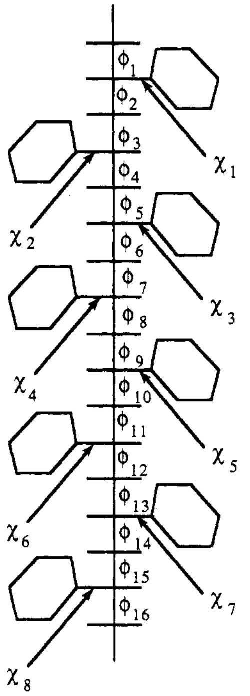

Figure 8. Definition of the sPS chain segment used in the MD simulation study.

in Table I where (θ_1,θ_2) = (112°,114°) yields lower conformational energies than (109.5°,109.5°) for both the T_4 and T_2G_2 structures. Figure 7 illustrates how the variations in (θ_1,θ_2), as reported in Table I, alter the geometry of the T_2G_2 conformation.

Lastly, some preliminary molecular dynamics, MD, simulations[14] were carried out for a four structural repeat unit segment of sPS. Figure 8 is a schematic illustration of the molecule considered in the MD studies. Trajectories were determined over 50 ps, starting with the T_2G_2 conformation at room temperature. The main finding of these studies is that the T_2G_2 conformation readily interconverts to the T_4 structure over the trajectory time interval. It should be noted that no T_4 to T_2G_2 transition was observed in the MD simulation. The estimated transition barrier to go from T_2G_2 to T_4 in the MD simulation is less than 3 kcal/mol.

The conformational interconversion between T_2G_2 and T_4 seems to be highly cooperative for pairs of adjacent backbone torsion angles. This is demonstrated in Figure 9 where the conformational profile of ϕ_5–ϕ_8 is plotted over time. It is seen that ϕ_6 undergoes a transition from G^+ to T which is quickly followed by the same conversion for ϕ_7. However, ϕ_5 and ϕ_8 are not perturbed by either of these transitions. The absolute difference of $|\phi_7 - \phi_6|$ versus time is plotted in Figure 9b. It is quite clear that ϕ_6 and ϕ_7 are coupled during the transitions, which, in composite, lasts for about 2–3 ps. No other conformations of sPS other than T_4 and T_2G_2 were found to persist over the trajectories.

Table II
Distribution of Backbone Bond Angles, θ_1 and θ_2, for the Last 40 ps of a MD Trajectory of 50 ps[a]

SRU[b]	θ_1	θ_2
1	113.3° ± 4.0°	116.9° ± 3.8°
	113.3 ± 4.1	115.2 ± 3.8
2	111.5 ± 3.8	114.8 ± 3.8
	111.5 ± 3.9	114.7 ± 3.8
3	113.7 ± 4.1	117.3 ± 3.6
	113.6 ± 4.0	116.3 ± 3.9
4	112.8 ± 4.2	116.6 ± 3.9
	113.1 ± 4.4	--

[a] The equilibrium bond angle for both θ_1 and θ_2 is 109.5°. [b] Structural repeat unit.

Table III
Fiber Axis Repeat Units/Identity Periods of sPS and Other Polymers in the T_4 and/or T_2G_2 Conformation

conformation	θ_1	θ_2	C, Å
T_4 (calcd)	109.5°	109.5°	5.03
T_4 (calcd)	112.0	114.0	5.12
sPS (exptl)			5.06[3], 5.06[4], 5.0[5]
polyethylene (exptl)[17]			5.09
sPP (T_4) (exptl)[7]			5.10
sPVC (T_4) (exptl)[18]			5.10
T_2G_2 (calcd)	109.5	109.5	7.11
T_2G_2 (calcd)	112.0	114.0	7.40
sPS (exptl)			7.5[4], 7.5[5]
sPP (T_2G_2) (exptl)[16]			7.40

The MD studies also suggest that the values for θ_1 and θ_2 should flip-flop between 112° and 114° down the polymer backbone. The initial equilibrium bond angle values for θ_1 and θ_2 were set at 109.5° in the MD studies. Nevertheless, as shown in Table II, the average distribution values realized over the last 40 ps of a trajectory are consistent with the (θ_1,θ_2) = (112°,114°) assignment.

Discussion

A comparison of the predicted stable conformations of sPS to the conformations of iPS indicates some similarities but more differences in the structures of the two polymers. A near all-trans conformation has been proposed for some gel formulations of iPS.[15,16] In particular, a 12_1 helix seems to best fit diffraction patterns of iPS gels. The T_2G_2 conformation is not a minimum energy conformation for iPS and seems to be a chain conformation more characteristic of syndiotactic vinyl polymers.[17] sPP adopts both a T_2G_2 and T_4 chain conformation as part of its crystalline polymorphism.[16,17] On the other hand, syndiotactic poly(vinyl chloride) (sPVC) only adopts an all-trans planar conformation in the crystalline state.[18] Table III summarizes the calculated and computed identity periods of sPS, sPP, polyethylene, and sPVC as a function of conformation.

It is not possible to predict whether T_4 or T_2G_2 or both conformations form stable crystal lattices from the intrachain conformational analyses reported here. However, these analyses, combined with the MD simulations, suggest that these are the only two ordered chain conformations available to sPS. Overall, our analyses support the chain conformations proposed for the experimental α and β crystalline phases of sPS, which are, respectively, T_4 and T_2G_2.[3-5]

The high cooperativity of conformational interconversion of adjacent G states to T states, see Figure 8, also leads

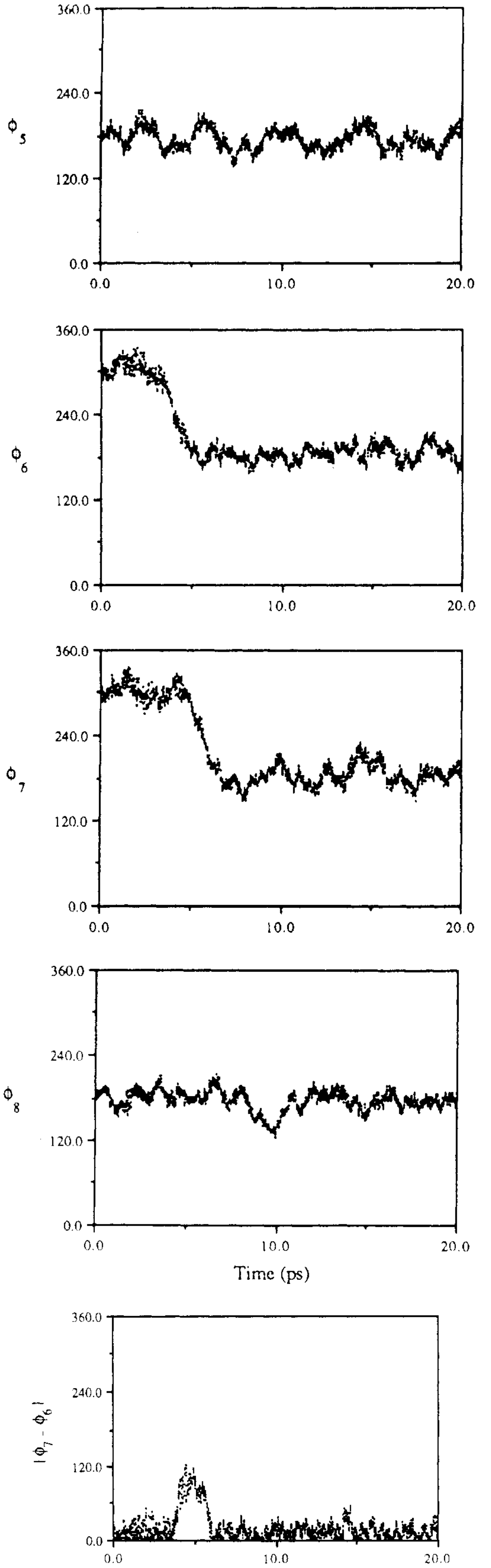

Figure 9. (a, top four) Torsion angle trajectory profiles for ϕ_5–ϕ_8. Note ϕ_6 and ϕ_7 each undergo a G^+ to T transition. (b, bottom) $|\phi_7 - \phi_6|$ plotted against time to illustrate the cooperativity of the G^+ to T transitions in these adjacent torsion angles.

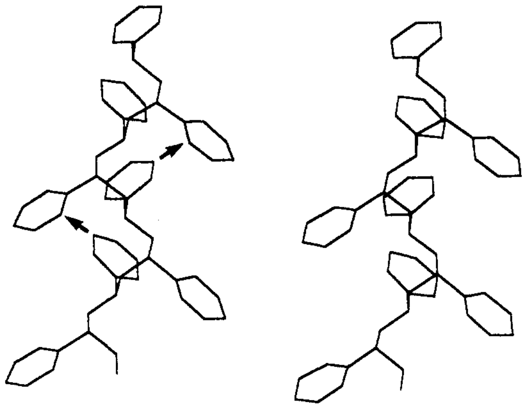

Figure 10. Steric violations for the E_2 interactions (see Table I) of T_2G_2 when (θ_1,θ_2) = (109.5°,109.5°). The arrows indicate the steric violations.

us to speculate that various distributions of T_4 and T_2G_2 structures are realized by high molecular weight sPS. The presence of a T_2G_2-to-T_4 transition and the absence of a T_4-to-T_2G_2 transition in the MD simulations are consistent with the observed thermal transition from the $\beta(T_2G_2)$ to the $\alpha(T_4)$ phase.[5] No α-to-β transition has been reported. The single-chain MD findings suggest that the β-to-α thermal transition may be largely governed by intrachain energetics. We cannot propose a reason for the apparent difficulty for a T_4-to-T_2G_2 transition. The conformational energy map in Figure 8 indicates the T_4 and T_2G_2 conformations should interconvert with a barrier of only 2–3 kcal/mol.

The choice of θ_1 and θ_2 is critical to the relative stability of the T_4 versus T_2G_2 conformation. If $\theta_1 = \theta_2 = 109.5°$, the T_2G_2 structure is destabilized by ring–ring interactions, which are defined by the arrows in Figure 10. This corresponds to the large destabilizing energy for E_2 in Table I. MD simulations suggest that θ_1 and θ_2 will tend toward (112°,114°) as a structural consequence even when 109.5° is selected as the force-field equilibrium bond angle for both backbone angles. In this regard, sPS is similar to iPS.

Electrostatic interactions do not play a particularly important role in the conformational behavior of sPS. Conformations that place the side-chain phenyl rings directly over one another in some periodic fashion, such as 3_1 and 4_1 helices, are moderately destabilized by side-chain–side-chain electrostatic interactions. Nonbonded dispersion interactions are the primary sources of conformational stability.

The conformational sensitivity of iPS to the choice of the nonbonded potentials points to the fact that computational conformational analyses cannot be treated as "blackbox" calculations. It is wise to see how sensitive conformational profiles are to the choice of force field. In this regard, the fidelity of a calculation on a particular molecule can be established by reproducing experimental properties of a homologue.

We are now in the process of using the T_4 and T_2G_2 conformations as starting structures in chain packing calculations. The CHAINPACK option in CHEMLAB-II[12] is being employed to establish minimum energy lattice structures. The results of these crystalline lattice prediction calculations will be the subject of our next paper.

Acknowledgment. This work was supported through a Cooperative Research Grant from the Dow Chemical Company and by funds from the Laboratory of Computer-Aided Molecular Modeling and Design at UIC. We are also grateful to Cray Research, Inc., for a University Research and Development Grant for computer time at the National Center for Supercomputing Applications at UIUC. All conformational energy calculations were done by using the CHEMLAB-II molecular modeling package.

The molecular dynamics calculations were done by using the MOLSIM system. Figures 5–7 and 10 were made by using the MicroChem molecular modeling software.

Registry No. sPS, 28325-75-9.

References and Notes

(1) Hopfinger, A. J. *Conformational Properties of Macromolecules*; Academic Press: New York, 1973.
(2) Orchard, B. J.; Tripathy, S. K.; Pearlstein, R. A.; Hopfinger, A. J. *J. Comput. Chem.* **1987**, *8*, 28.
(3) Ishihara, N.; Seimiya, T.; Kuramoto, M.; Ubi, M. *Macromolecules* **1986**, 2464.
(4) Chatani, Y.; Fujii, Y.; Shimane, Y.; Ijitsu, T. *Polym. Prepr. Jpn.* **1988**, *37*, 26-0-12.
(5) Kobayashi, M.; Nakaoki, T.; Uoi, M. *Polym. Prepr. Jpn.* **1988**, *37*, 26-0-20.
(6) Corradini, P.; Natta, G.; Ganis, P.; Temussi, P. A. *J. Polym. Sci. Part C* **1967**, *16*, 2477.
(7) (a) Natta, G.; Peraldo, M.; Allegra, G. *Makromol. Chem.* **1966**, *9*, 181. (b) Tadokoro, H.; Kobayashi, M.; Kobayashi, S.; Yasufuku, K.; Mori, K. *Rep. Prog. Polym. Phys. Jpn.* **1966**, *9*, 181.
(8) Hopfinger, A. J. *J. Med. Chem.* **1985**, *28*, 1133.
(9) Yoon, D. Y.; Sundarajan, P. R.; Flory, P. J. *Macromolecules* **1975**, *8*, 776.
(10) Natta, G.; Corradini, P.; Bassi, I. W. *Nuovo Cimento, Suppl.* **1960**, *15*, 68.
(11) Pople, J. A.; Santry, D. P.; Segal, G. A. *J. Chem. Phys.* **1965**, *43*, 5129. Pople, J. A.; Segal, G. A. *Ibid.* **1965**, *43*, 5136; **1966**, *44*, 3289.
(12) Pearlstein, R. A. *CHEMLAB-II Users Guide*; Chemlab: 1780 Wilson Dr., Lake Forest, IL 60045, Jan 1988.
(13) Allinger, N. L.; Yuh, Y. H. Operating Instructions for MM2 and MMP2 Program—1977 Force Field. *QPCE* **1980**.
(14) McCammon, J. A.; Harvey, S. *Dynamics of Proteins and Nucleic Acids*; Cambridge University Press: London, 1987.
(15) Girolamo, M.; Keller, A.; Miyasaka, K.; Overbergh, N. *J. Polym. Sci., Polym. Phys. Ed.* **1976**, *14*, 39.
(16) Atkins, E. D. T.; Isaac, D. H.; Keller, A.; Miyasaka, A. *J. Polym. Sci., Polym. Phys. Ed.* **1977**, *15*, 211.
(17) Tadakoro, H. *Structure of Crystalline Polymers*; Wiley-Interscience: New York, 1979.
(18) Natta, G.; Corradini, P. *J. Polym. Sci.* **1956**, *20*, 251.

An Off-Lattice Constant-Pressure Simulation of Liquid Polymethylene

Richard H. Boyd

Department of Materials Science and Engineering and Department of Chemical Engineering, University of Utah, Salt Lake City, Utah 84112. *Received September 12, 1988*

ABSTRACT: An off-lattice constant-pressure Monte Carlo simulation has been carried out for a model of liquid polymethylene. Reptation was used as the Monte Carlo move. Methylene units were represented by united atom beads with nonbonded potentials of interaction between them. Intramolecular torsional potentials were used, but the molecules were rigid with respect to bond stretching and bending. The system consisted of 32 chains of 24 methylene units each. *PVT* data were generated over the ranges 300–500 K and 1–1000 atm. The equilibrium volume at 1 atm is in good agreement (2%) with that for tetracosane. The thermal expansion at 1 atm and the isothermal compressibility at 450 K agree well with experiment for polyethylene. Harmonic vibrational analysis was carried out separately for representative configurations of the molecules in the system and the resulting calculated vibrational heat capacity added to the intermolecular heat capacity from the simulation to arrive at the melt constant-pressure heat capacity. The latter is in agreement with experiment. The gauche–trans ratio and the mean-square end-to-end distance are found to be independent of pressure. The latter is also found to be in agreement with the rotational isomeric state model.

It is well-known that the simulation of molecular packing in dense polymer fluids is an extraordinarily difficult problem. Yet the ability to describe in detail the packing under these circumstances is of paramount importance in the general area of structure-property prediction and correlation in polymeric materials. The difficulty in simulation lies, of course, in the molecular connectivity. In a polymer melt, the molecules are visting conformational space by virtue of many cooperative bond rotations. The slow physical time scale of these bond rotations, 10^{-6} s or longer in most applications of interest, precludes the direct attack via molecular dynamics (MD) where the basic time step is $\sim 10^{-15}$ s. Use of Monte Carlo methods in the equilibrium situation is not straightforward because of the difficulty in finding elementary moves that lead to exploring efficiently the intramolecular conformational space under the restrictions of the intermolecular packing. Lattice methods have been extensively applied to Monte Carlo simulation of polymer fluids. Although sacrifice in physical realism is made, they are inherently faster than an unrestricted or off-lattice method. The problem of finding acceptable moves in conformational space in the presence of dense intermolecular packing is exacerbated on the lattice. However, very significant progress has been made as the result of the realization that reptational moves provide a means of sampling conformational space that is efficient enough to allow simulation of molecules of reasonable length in dense, but not fully occupied, lattices.[1-4] There has been some work off-lattice. Reptational moves have been employed in a fluid of chains consisting of harmonically connected beads.[5] There is one study where the reptational method has been used off-lattice and a realistic torsional potential employed.[6] Although the results were not extensive, the method appears quite successful.

Another weakness of simulations with respect to realism is the fact that constant volume has been used. The structural or molecular packing changes in the polymeric melt with temperature could be very important in the context of vitrification and property change in general. However, the changes under constant volume simulation will be very different from the constant pressure conditions of nearly all experiments. Motivated by a desire to simulate a system realistic enough from a molecular point of view to be able to make property predictions for comparison with experiment, we have investigated here the